



Cell-Lineage Guided Mass Spectrometry Proteomics in the Developing (Frog) Embryo

Aparna B. Baxi^{1,2}, Leena R. Pade¹, Peter Nemes^{1,2,*}

¹Department of Chemistry & Biochemistry, University of Maryland, College Park, MD 20742, USA

²Department of Anatomy & Cell Biology, The George Washington University, Washington, DC 20052, USA

Abstract

Characterization of molecular events as cells give rise to tissues and organs raises a potential to better understand normal development and design efficient remedies for diseases. Technologies enabling accurate identification and quantification of diverse types and large numbers of proteins would provide still missing information on molecular mechanisms orchestrating tissue and organism development in space and time. Here, we present a mass spectrometry-based protocol that enables the measurement of thousands of proteins in identified cell lineages in *Xenopus laevis* (frog) embryos. The approach builds on reproducible cell-fate maps and established methods to identify, fluorescently label, track, and sample cells and their progeny (clones) from this model of vertebrate development. After sampling cellular contents using microsampling or isolating cells by dissection or fluorescence-activated cell sorting, proteins are extracted and processed for bottom-up proteomic analysis. Liquid chromatography and capillary electrophoresis are used to provide scalable separation for protein detection and quantification with high-resolution mass spectrometry (HRMS). Representative examples are provided for the proteomic characterization of neural-tissue fated cells. Cell-lineage-guided HRMS proteomics is adaptable to different tissues and organisms. It is sufficiently sensitive, specific, and quantitative to peer into the spatio-temporal dynamics of the proteome during vertebrate development.

SUMMARY:

Here we describe a mass spectrometry-based proteomic characterization of cell lineages with known tissue fates in the vertebrate *Xenopus laevis* embryo.

*Corresponding author: Peter Nemes (nemes@umd.edu).

A complete version of this article that includes the video component is available at <http://dx.doi.org/10.3791/63586>.

DISCLOSURES

The authors declare no competing interests.

SUPPLEMENTARY INFORMATION

The HRMS-MS/MS proteomics data and related processing files were deposited to the ProteomeExchange Consortium via the PRIDE⁶⁰ partner repository with the data set identifier PXD030059.

Keywords

cell lineage tracing; dissection; liquid chromatography; capillary electrophoresis; mass spectrometry; proteomics; development; *Xenopus laevis*

INTRODUCTION:

Our understanding of cell differentiation and the genesis of tissues and organs is the result of decades of elaborate targeted screens of genes and their products. Increasing our knowledge of all the biomolecules and their quantities during important cellular events would help unravel molecular mechanisms that control the spatial and temporal patterning of the vertebrate body plan. Technologies enabling molecular amplification and sequencing are now able to routinely report on large numbers of genes and transcripts, supporting hypothesis-driven studies in basic biological and translational research. To understand developing systems, a complex relationship between transcription and translation advocates for direct analysis of multiple proteins and their post-translational modifications. Global proteomics using *in vitro* biological systems, such as induced pluripotent stem cells, began to delineate mechanisms of tissue induction^{1,2}. In complex organisms, such as the vertebrate embryo, development relies on morphogen gradients in the context of space and time³. It follows that gaining knowledge of proteomic changes as cells differentiate to form specialized tissues, such as neural tissues, offers a key to unlock molecular programs controlling normal and defective development and guide next-generation therapeutics.

The vertebrate South African clawed frog (*Xenopus laevis*) is a well-established model in cell and developmental, neuro-, and regenerative biology. Sir John Gurdon's 2012 Nobel Prize in Physiology or Medicine^{4,5} for the discovery of pluripotency of the somatic nucleus highlighted the importance of this model for discoveries in basic and translational studies. *Xenopus* embryos develop externally to the mother, thus facilitating direct manipulation of cells, cell clones, and gene expression over various stages of development. Asymmetrical pigmentation and stereotypical cell divisions enabled the charting of reproducible fate maps from the 16-⁶ and 32-cell^{7,8} stage embryo. For high-resolution mass spectrometry (HRMS) based proteomics, additional advantages of the model include relatively large size (~1 mm in diameter), which yields abundant protein content for analysis (~130 µg in early cleavage-stage embryos, ~10 µg of protein content in single cells of the 16-cell embryo)^{9,10}.

At present, HRMS is the leading technology of choice for detecting proteins. This technology enables direct, sensitive, and specific detection and quantification of multiple, usually thousands, of different proteins¹¹. Bottom-up proteomics by HRMS involves a series of interconnected steps. Following extraction from the cell/tissue sample, proteins are usually digested with a proteolytic enzyme, such as trypsin (bottom-up proteomics). The resulting peptides are separated based on their different physicochemical properties, including hydrophobicity (reversed-phase liquid chromatography, LC), net charge (ion-exchange chromatography), size (size exclusion chromatography), or electrophoretic mobility (capillary electrophoresis, CE). Peptides are then charged (ionized), typically using electrospray ionization (ESI), and peptide ions are detected and sequenced via gas-phase

fragmentation by tandem HRMS. The resulting peptide data are mapped to the proteome of the organism being studied. With protein-specific (proteotypic) peptide ion signal intensity correlating with concentration, protein quantification can be performed label-free or label-based (multiplexing quantitation). HRMS proteomics yields a rich resource of information on the molecular state of the system under study, allowing for the generation of hypotheses and follow-up functional studies.

The protocol presented here enables HRMS-based quantification of large numbers of proteins in identified cells/tissues in developing *X. laevis* embryos. The approach builds on accurate cell identification, reproducible cell fate maps, and established methodologies to track cell lineages in this biological model⁶⁻⁸. As shown in Figure 1, we study proteomes from single cells by employing whole-cell dissection or capillary microsampling to aspirate cellular content. Monitoring the lineage of a cell permits us to study the spatiotemporal evolution of the proteome as cells form tissues during gastrulation. The cell progeny is fluorescently marked by injecting a fluorophore conjugated to inert dextran or mRNA for fluorescent protein (e.g., green fluorescent protein, or GFP). The labeled progeny is isolated at desired developmental time points. During gastrulation, cell clones that are tightly clustered may be isolated by dissection. After gastrulation, cell clones may be distributed within the embryo owing to migratory movements and can be isolated from dissociated tissues by fluorescence-activated cell sorting (FACS). Proteins in these cells and tissues are measured via bottom-up proteomics employing HPLC or CE for separation and ESI tandem HRMS for identification. Cell-lineage-guided HRMS proteomics is scalable to different cell sizes and lineages within the embryo and is specific, sensitive, and quantitative. Through select examples shown here, we also demonstrate this protocol to be scalable and broadly adaptable to different types of cells and cell lineages.

PROTOCOL:

All protocols ensuring the humane maintenance and handling of *Xenopus laevis* adult frogs were approved by the Institutional Animal Care and Use Committee at the University of Maryland, College Park (Approval numbers R-DEC-17-57 and R-FEB-21-07).

1. Prepare the solutions

1.1. For embryology

1.1.1. Prepare 1x, 0.5x, and 0.2x Steinberg's solution (SS), then autoclave them (120 °C for 20 min) to sterility following standard protocols¹².

1.1.2. Prepare 3% (w/v) Ficoll in sterilized 1x SS following standard protocols¹².

1.1.3. For dejellying, freshly prepare 2% (w/v) cysteine solution and adjust its pH to 8 by adding 10 M sodium hydroxide solution dropwise.

CAUTION: Exposure to cysteine can cause skin and respiratory damage. Sodium hydroxide is a corrosive that can cause serious damage to skin and eyes upon direct exposure. Use appropriate personal protective equipment (PPE) when handling these chemicals, such as gloves and a laboratory coat.

1.1.4. For the lineage tracer, prepare 0.5% (v/v) of a fluorescent dextran in sterile deionized water. Alternatively, prepare a solution of 0.2 $\mu\text{g}/\mu\text{L}$ of mRNA for fluorescent proteins in sterile deionized water (e.g., GFP).

1.1.5. To dissociate cells, prepare Newport 2.0 buffer containing 0.1 M sodium isethionate, 20 mM sodium pyrophosphate, and 10 mM CAPS, then bring its pH to 10.5¹³.

CAUTION: Exposure to sodium pyrophosphate can cause skin and eye irritation. Use appropriate PPE when handling these chemicals.

1.2. For bottom-up proteomics

1.2.1. Prepare the cell lysis buffer to include: 250 mM sucrose, 1% nonidet P-40 substitute (w/v), 20 mM Tris-HCl, 5 mM EDTA, 10 μM cytochalasin D, and 10 μM combretastatin 4A. Prepare a stock of 10% (w/v) sodium dodecyl sulfate^{14,15}.

NOTE: Tris-HCl was chosen to minimize HEPES contamination during nano-flow LC (nanoLC)-HRMS.

CAUTION: Exposure to nonidet P-40 substitute can cause skin irritation. Cytochalasin D is teratogenic if consumed and combretastatin is acutely toxic upon direct exposure. Use appropriate PPE when handling these chemicals.

1.2.2. To separate peptides by CE, prepare the following solvents (v/v): Sample solvent, 75% acetonitrile (ACN) containing 0.05% acetic acid (AcOH) in water; sheath solution, 10% ACN containing 0.05% AcOH in water; background electrolyte (BGE), 25% ACN containing 1 M formic acid (FA) in water.

CAUTION: AcOH and FA are toxic when inhaled or consumed and can cause serious skin and eye damage upon direct exposure. Use appropriate PPE when handling these chemicals.

1.2.3. To separate peptides by reversed-phase nanoLC, prepare (v/v): Mobile phase A (aqueous), water containing 0.1% FA; mobile phase B (organic), 0.1% FA in ACN.

NOTE: All mixtures should be prepared using LC-HRMS grade solvents to minimize chemical interferences during HRMS detection.

2. Prepare the tools for microinjection and dissection

2.1. To gently move and orient embryos, make hair loops by fixing clean hair into a Pasteur pipette as described elsewhere¹⁶.

2.2. For microinjection, fabricate needles by pulling borosilicate capillaries (1 mm/500 μm outer/inner diameter) using a pipette puller as described elsewhere¹⁶.

NOTE: Here, a P-1000 Pipette Puller with the following settings was used for fabricating needles: heat, 495; pull, 30, velocity, 60; time, 150; pressure, 200.

2.3. With observation under a stereomicroscope, cut the tip of the capillary using a pair of sharp forceps to essentially fabricate the capillary into a (micro)needle (e.g., Dumont #5)¹⁶.

CAUTION: Pulled capillaries are very sharp and should be handled with care.

NOTE: The tip of the needle should be sharp enough (outer diameter 10–15 μm) to be able to pierce the cell with minimal damage to the cell membrane so that the intracellular content does not leak out and the cell can heal and continue to be viable.

2.4. To hold embryos during microinjection, prepare wells in a clay-filled dish. In a 15 mm Petri dish, imprint ~1 mm diameter x ~0.5 mm deep wells into non-toxic plasticine clay as described elsewhere¹⁶.

2.5. For microdissection, prepare agarose-coated dishes. Make 2% agarose in 1x SS and autoclave it to sterilize the solution (120 °C for 20 min). Fill 60 mm Petri dishes halfway, and let the plates solidify. Make ~1 mm diameter x ~0.5 mm deep wells using a balled Pasteur pipette tool as described previously¹⁶.

3. Isolate the cell lineage

NOTE: The following steps are performed to isolate identified single cells and/or their descendent cell lineages. Usually, the embryo is cultured to the 16- or 32-cell stage, where the tissue fates of each cell are reproducibly mapped^{6,7,17}. The embryonic cells are identified based on morphology, location, and in reference to their fate maps. For single-cell analysis, identified cells are isolated by manual dissection, or their intracellular contents are collected into a capillary pipette and deposited in 5 μL of 0.5 mM ammonium bicarbonate. The resulting sample is stored at $-80\text{ }^{\circ}\text{C}$ until analysis (Figure 1)¹⁸⁻²¹. For cell lineage analysis, identified cells are injected with a lineage tracer, and their subsequent clones are isolated at key stages of development (e.g., during gastrulation to study tissue induction, following neurulation to study tissue commitment). In what follows, steps are outlined to fluorescently label the lineage of identified cells for isolation by dissection or FACS.

3.1. Culture the embryos

3.1.1. Obtain embryos via natural mating or *in vitro* fertilization (IVF) following established protocols¹².

NOTE: Natural mating is logistically simpler, spares the adult male frogs, and yields embryos at different developmental stages, whereas IVF provides developmentally synchronized embryos for experiments that require accurate staging.

3.1.2. Dejelley the embryos. Remove the jelly coat surrounding the embryos via treatment with the dejellying solution as described elsewhere^{12,16}.

NOTE: Microinjections and dissection require access to the cells and tissues, necessitating dejellying in *X. laevis* embryos.

3.1.3. Select 2-cell embryos with stereotypical pigmentation^{16,22}.

NOTE: This step is important to ensure accuracy and reproducibility in the identification of the cell and its lineage.

3.1.4. Culture embryos to the desired developmental stage. Transfer the dejellied embryos to a Petri dish containing 1x SS and incubate them between 14–25 °C to control the speed of development.

NOTE: The temperature dependence of development is reproducible and charted for *X. laevis*, available on Xenbase²³ (www.xenbase.org). Culturing batches of embryos at different temperatures allows for staggering developmental stages. Doing so helps distribute the number of embryos available at a given time for experimentation.

3.1.5. Monitor the cleavage pattern of embryos and select embryos with stereotypical pigmentation and cleavage patterns for microinjection¹⁶.

NOTE: When selecting 16- and 32-cell embryos, ensure that the cell cleavages are symmetrical for reproducible lineage tracing.

3.2. Label the cell(s) of interest

3.2.1. Set up the injection needle containing the lineage tracer solution. Mount the microinjection needle into a micropipette holder controlled by a multi-axis micromanipulator.

3.2.2. Connect the micropipette holder to a microinjector. Fill the needle with the lineage tracer by applying negative pressure as described elsewhere¹⁶. Figure 1A exemplifies our setup.

3.2.3. Calibrate the needle. Adjust the size of the needle tip and injection time to deliver ~1 nL of the lineage tracer solution, measured in (mineral) oil following a protocol available elsewhere¹⁶.

NOTE: Capillaries with a wider tip tend to damage the cell membrane, causing subcellular contents and the injected lineage tracer to leak out, whereas capillaries with smaller tips are prone to clogging. Capillaries with ~10 µm tip outer diameter are ideal, requiring a 40 psi pressure pulse over ~300 ms to deliver ~1 nL.

3.2.4. Flood the microinjection clay dish with the 3% Ficoll solution, transfer ~10 embryos to the clay dish using a transfer pipette. Use a hair loop to guide each embryo into a well and gently position them so that the targeted cell of interest is at a right angle to the microneedle.

3.2.5. Identify the precursor cell of the lineage of interest following the *X. laevis* tissue fate maps. For example, Figure 1 demonstrates the labeling of neural ectodermal clones based on the injection of its precursor cells in 32-cell embryos (left and right D₁₁₁ cells).

NOTE: Detailed fate maps for the 16-⁶ and 32-cell^{7,8} embryos are available in an interactive platform via Xenbase²³. It is important to ensure stereotypical pigmentation and cleavages on embryos when using them for lineage-tracing experiments.

3.2.6. Inject the cell(s) of interest with ~1 nL of the fluorescent dextran or ~200 pg of mRNA as described earlier¹⁶.

NOTE: Use dextran conjugates that are 10,000–40,000 MW. Smaller dextran conjugates could pass through gap junctions, whereas larger dextran conjugates may not diffuse evenly into the injected cell. Plan to inject cells in ~10 embryos to have sufficient tissues for proteomic analyses.

3.2.7. Confirm the success of cell labeling under a stereomicroscope. Ensure that only the intended cell is injected. Discard embryos containing injured or incorrectly labeled cells following institutional policies.

NOTE: Because *X. laevis* is invasive in many non-natural environments, embryos may be frozen to ensure lethality before discarding the embryos.

3.3. Isolate the labeled cell progeny

3.3.1. Transfer the injected embryos to 0.5x SS in a Petri dish and culture them between 14–25 °C until the desired developmental stage is reached.

NOTE: Consult established protocols to stage embryos reported on Xenbase.

3.3.2. Transfer 3–5 embryos to an agar dish with 0.2x SS solution for microdissections.

NOTE: Reducing the salt concentration of SS solution from 0.5x to 0.2x helps separate cells during dissection.

3.3.3. Use two sharpened forceps to gently remove the vitelline membrane surrounding the embryo.

NOTE: To spare the clone of interest from damage, peel the membrane from the opposite side of the fluorescently labeled clone.

3.3.4. Isolate the labeled clone by manual dissection (steps 3.3.5–3.3.6) or FACS (steps 3.3.7–3.3.8) as follows.

3.3.5. Use forceps to dissect the labeled clone from the embryo.

NOTE: Other tools such as microsurgical scissors, tungsten needles, or eyebrow hair knives can be used for dissection of the labeled clone, as detailed elsewhere¹⁶.

3.3.6. Collect the dissected tissue with a 0.5–10 µL pipette and deposit them into a microcentrifuge vial. Using a transfer pipette, aspirate the media surrounding the collected tissue to limit salts in the sample, which interfere with HRMS analysis in later steps.

NOTE: Use vials that minimize protein adsorption onto plastic surfaces to minimize protein losses on vial surfaces during later steps of the workflow.

3.3.7. Transfer ~5–8 devitellized embryos into each well of a 12-well plate containing ~5 mL of Newport 2.0 buffer. Dissociate the embryos by nutating the plate at 80 rpm for 20–30 min at room temperature¹³.

NOTE: Embryos/larvae older than stage 22 have abundant extracellular matrix proteins, making dissociation into separate cells difficult. Additional enzymatic approaches can be adapted for dissociating tissues from older embryos as described elsewhere²⁴.

3.3.8. Purify the fluorescently labeled cells from the suspension using FACS as described elsewhere²⁴.

3.3.9. Pellet cells by centrifugation and discard the supernatant.

NOTE: Use low centrifugation speed ($400 \times g$) and temperature ($4\text{ }^{\circ}\text{C}$) to prevent cell lysis. If using bovine serum albumin (BSA) for FACS, wash the cell pellet to reduce BSA interference during HRMS detection. Gently resuspend the cells in 1x phosphate buffered saline (PBS) and centrifuge again to pellet rinsed cells. Remove the supernatant PBS liquid.

3.3.10. Swiftly freeze the isolated cells by placing the sample vial on dry ice or liquid nitrogen.

NOTE: Keep the samples (tissues or cells) cooled (e.g., on ice) during processing steps. Freeze the cells with as little media around the sample as possible to facilitate downstream processing.

3.3.11. Store the samples at $-80\text{ }^{\circ}\text{C}$ until HRMS analysis.

4. Analyze the proteins by mass spectrometry

NOTE: Proteomic characterization of the isolated tissues or cells is based on a series of established steps in HRMS. Figure 2 illustrates the steps of the bioanalytical workflow. The sample collection protocol used here is compatible with bottom-up¹¹, middle-down²⁵, or top-down²⁶ workflows of proteomics. In what follows, the bottom-up strategy used in this study is described, which has proved to be sensitive, quantitative, and adaptable to diverse types of mass spectrometers. After extracting and enzymatically digesting proteins, the resulting peptides are separated, followed by HRMS analysis.

4.1. Process the tissues/single cells

4.1.1. For single-cell analysis by CE, heat the sample to $60\text{ }^{\circ}\text{C}$ for ~ 15 min to denature proteins, then equilibrate the sample to room temperature (RT, ~ 5 min)^{18,21}.

NOTE: Unlike during working with tissues, the reduction and alkylation steps are skipped to limit protein losses during sample preparation from single cells. Filter-aided sample preparation (FASP)^{27,28}, other single pot strategies²⁹, and microfluidic approaches³⁰ can be adopted to minimize protein losses during sample preparation.

4.1.2. For analysis by nanoLC, lyse up to 5 dissected tissues in $50\text{ }\mu\text{L}$ of lysis buffer ($\sim 100\text{ }\mu\text{g}$ of total protein). Facilitate the process by pipetting the sample up and down a few times.

4.1.3. Incubate the lysate at $4\text{ }^{\circ}\text{C}$ for 10 min, then pellet the cell debris and yolk platelets by centrifugation at $4,500 \times g$ at $4\text{ }^{\circ}\text{C}$. Transfer the supernatant into a clean microcentrifuge vial and add 10% SDS to obtain a final concentration of 1% SDS in the lysate (v/v).

4.1.4. For tissues, follow steps 4.1.5–4.1.7.

4.1.5. Add 0.5 M dithiothreitol to the lysate to obtain a final concentration of ~25 mM (e.g., 2.5 μ L of 0.5 M dithiothreitol to 50 μ L of lysate) and incubate the lysate for 30 min at 60 °C to chemically reduce disulfide bonds in proteins.

4.1.6. Add 0.5 M iodoacetamide to obtain a final concentration of ~75 mM in the lysate and incubate the mixture for 15 min at RT in the dark (Figure 2).

4.1.7. Add 0.5 M dithiothreitol, same as the initial volume (e.g., 2.5 μ L of 0.5 M dithiothreitol to 50 μ L of lysate) to quench reactants remaining from the alkylation reaction.

CAUTION: Iodoacetamide and dithiothreitol can cause serious skin and eye damage upon direct exposure. Use appropriate PPE when handling these chemicals.

4.1.8. Purify proteins via precipitation. Chloroform-methanol-based precipitation performs well³¹. This protocol is also adaptable to other types of precipitation approaches³².

NOTE: For single-cell analysis, where protein losses are of concern, skip the precipitation step for CE-HRMS.

4.1.9. Dry the protein precipitate in a vacuum concentrator (4–37 °C), then resuspend the extracted proteome in 50 μ L of 50 mM ammonium bicarbonate. Estimate the protein concentration using a total-protein colorimetric assay to determine the amount of enzyme required for digestion (e.g., bicinchoninic acid protein assay).

4.1.10. Digest the proteins to peptides. Add trypsin (1 μ g/ μ L stock) to obtain a protease:protein ratio of 1:50 and incubate the mixture at 37 °C for up to 5 h for single-cell samples and up to 14 h for tissue samples. Consult vendor-specific recommendations for the reaction.

NOTE: Digestion with trypsin for longer than 14 h or higher concentrations may introduce cleavages that are nonspecific to the sequence of the protein, thus challenging protein identifications³³.

4.1.11. Quantify the total peptide concentration using a colorimetric assay.

4.1.12. **OPTIONAL:** For multiplexing quantification, tag the peptides from each sample with a different isobaric mass tag following vendor-specific instructions. Mix the barcoded peptides in equal proportions per peptide sample.

NOTE: Ensure accurate labeling and mixing to avoid quantitative biases. For quantity-limited samples or single-cell samples, a TMT-based carrier channel composed of pooled tissues/cells can be included to minimize sample losses during subsequent separation steps and to boost the sensitivity of lower abundant proteins³⁴.

4.1.13. **OPTIONAL:** Desalt peptides to remove salts and contaminants (e.g., unreacted isobaric mass tag reagents) on a C18 reversed-phase spin column/tip to protect the LC-MS system.

4.1.14. OPTIONAL: Fractionate (e.g., medium- or high-pH reversed-phase fractionation) the peptide mixture for deeper detection of the proteome via manual or automatic platforms. Use C18 stationary phase containing tips to fractionate low amounts (1–10 μg) of peptide digests.

4.1.15. Dry the peptide mixture at 60 °C in a vacuum concentrator.

4.1.16. Store the peptide mixture at –80 °C until measurement.

4.2. Separate the Peptides

NOTE: After extracting and enzymatically digesting proteins, the resulting peptides are separated by nanoLC or CE and ionized by ESI for sequencing by tandem HRMS. Reversed-phase nanoLC separation is ideal for peptides amassing ~150 ng to ~1 μg per analysis. CE provides complementary sensitivity for peptides ranging from femtograms to <100 ng. Various custom-built and commercial CE-ESI interfaces allow for ready coupling of CE to HRMS with robust performance³⁵ and are increasingly used for single-cell analysis^{18,36,37}.

4.2.1. To separate using CE, follow steps 4.2.2–4.2.7.

NOTE: In what follows, the use of our custom-built CE platform for measuring the peptides is described. Protocols to build and use this CE instrument were provided earlier³⁸, along with a visualized experiment on usage for small molecules²⁰. Alternatively, these measurements can be performed on a commercial CE system, such as the AB SCIEX CESI, Agilent 7100, or equivalent.

4.2.2. Reconstitute the protein digest in 1–2 μL of the sample solvent, vortex to mix the sample, and centrifuge it at 10,000 $\times g$ for 2 min to pellet cell debris.

NOTE: Removal of the cell debris minimizes the likelihood of clogging the CE capillary, thus prolonging the lifetime of the separation system and boosting measurement throughput.

4.2.3. Initialize the CE-ESI instrument by flushing the CE capillary with the BGE.

4.2.4. Validate instrumental performance using a known standard (e.g., cytochrome C or BSA digest, angiotensin peptides).

NOTE: Evaluating the instrument in terms of mass accuracy, detection sensitivity, reproducibility, and linear dynamic range of quantification is recommended before measuring precious samples. Additional notes on validation and troubleshooting of CE-ESI-MS performance are listed elsewhere^{18,20,38}.

4.2.5. Inject ~1–10 nL of the sample into the CE separation capillary.

NOTE: This study uses ~1 m long fused silica capillary (40/110 μm inner/outer diameter) with the electrokinetically pumped sheath-flow setup. Commercial CE instruments usually require the presentation of 5–10 μL of sample in a microvial for injection. The custom-built CE platform^{18,38} is compatible with ~250 nL to 1 μL of sample deposited into a sample-loading microvial.

4.2.6. Transfer the inlet end of the CE separation capillary into the BGE.

4.2.7. Start electrophoretic separation by gradually ramping the CE separation voltage from Earth ground (e.g., stepwise over 1 min). Potentials of 20–28 kV with current below $\sim 10 \mu\text{A}$ ensure stable and reproducible instrumental performance for analysis.

4.2.8. To separate using nanoLC, follow steps 4.2.9–4.2.12.

4.2.9. Resuspend the peptide sample in Mobile Phase A. The concentration of the sample and its volume for injection depends on the available LC system and column. In this study, $\sim 250 \text{ ng} - 1 \mu\text{g}$ of protein digest is injected in 1–20 μL of sample volume on a C18 packed-bed column (75 μm inner diameter, 2 μm particle size with 100 \AA pores, 25 cm length separation column).

4.2.10. Transfer the sample into an LC vial.

NOTE: Ensure that there are no air bubbles in the vial, which may damage the analytical column. Vials with inserts could be used for low-volume tissue or single-cell samples.

4.2.11. Load $\sim 200 \text{ ng}$ to 2 μg of peptide sample onto the C18 analytical column.

NOTE: Optionally, the peptides can be loaded on a trap column for desalting prior to analytical separation. For example, a C18 trap column with 0.1 mm inner diameter, 5 μm particle size, 100 \AA pore size, 20 mm length. Desalt peptides with 100% buffer A at a flow rate of 5 $\mu\text{L}/\text{min}$ for 5 min before the separation gradient begins.

4.2.12. Separate the peptides using gradient elution. At a 300 nL/min flow rate, the 120-min gradient used in this study is as follows: 0–5 min 2% B, 5–85 min 2–35% B, 86–90 min 70% B, 91–120 min 2% B.

4.3. Ionize the peptides by ESI

NOTE: After separation, peptides are ionized. The effluent from the CE or nanoLC capillary is most typically coupled into an ESI source for ionization. Micro-flow (blunt-tip) and nano-flow (tapered-tip³⁹ and electrokinetic pumped sheath-flow³⁶ design) CE-ESI interfaces for ultrasensitive detection have been developed previously.

4.3.1. Supply the separating peptides into an electrospray ion source for ionization using a commercial or custom-built ESI interface. For single-cell CE-ESI-MS analysis in *Xenopus* embryos, use an electrokinetically pumped low-flow interface wherein the CE capillary outlet is enclosed in a pulled borosilicate emitter.

4.3.2. Check the liquid flow through the electrospray emitter using a camera and visually inspect the setup for possible leaks (e.g., EO-2018C, Edmund Optics Inc., Barrington, NJ).

4.3.3. Set the electrospray voltage to $\sim 2.5 \text{ kV}$ to start the ESI source (vs. Earth ground).

4.3.4. Ensure a stable nanospray for HRMS analysis by monitoring the total ion current. Adjust the electrospray voltage and distance of the emitter to the HRMS inlet to achieve a stable spray (<15% relative standard deviation in total intensity).

4.4. Detect the peptides

NOTE: Detection of peptides follows different instrumental considerations for isobaric mass tagged and untagged peptides and depends on the type of available mass spectrometer. This study uses an orbitrap tribrid mass spectrometer according to the following steps.

4.4.1. Acquire MS¹ events with the settings: Analyzer, orbitrap; Spectral resolution, 120,000 full width at half maximum (FWHM); maximum injection time (IT), 50 ms; automatic gain control (AGC), 4×10^5 counts; microscans, 1.

4.4.2. To sequence peptides, fragment precursor ions for detection in the ion trap analyzer using the settings: fragmentation mode, higher energy collision dissociation (HCD); collision gas, nitrogen; collision energy, 32% normalized collision energy (NCE); maximum IT, 70 ms; AGC, 1×10^4 counts; microscans, 1.

4.4.3. OPTIONAL: Quantify TMT tagged peptides at the MS² level using tandem/multistage HRMS (MS²/MS³) following steps 4.4.4–4.4.6. For MS³ employing synchronous precursor selection, the typical instrumental settings are as follows. Single-stage (MS¹) scans surveying the most abundant ions are dissociated via data-dependent acquisition using the parameters: MS² fragmentation mode, collision induced dissociation (CID); collision gas, helium; collision energy, 35% NCE; analyzer for fragment ions, ion trap following settings: maximum IT, 50 ms; AGC, 5×10^4 counts; microscans, 1. Select the top 10 most intense MS² fragment ions and fragment them with HCD in nitrogen (65% NCE). Detect MS³ fragment ions using the following settings: Orbitrap resolution 15,000 FWHM, maximum IT, 120 ms; AGC, 1×10^5 counts; microscans, 1. NOTE: Different MS acquisition methods and parameters can be used for tagged samples following vendor recommendations as described elsewhere^{11,40}.

4.5. Analyze the data

NOTE: Proteins are identified and quantified using advanced bioinformatic packages. The fidelity of identifications is calculated using a decoy database, expressed as the false discovery rate (FDR) at the level of peptides and proteins.

4.5.1. Process the data using commercial or open-source software packages (reviewed in reference⁴¹). Match the raw data against a database that was prepared by concatenating the *Xenopus* proteome 9.2 with the mRNA-derived PHROG database⁴².

NOTE: The search parameters are: digestion enzyme, trypsin; missed cleavages, up to 2; variable modification, methionine oxidation; static modification, cysteine carbamidomethylation; precursor mass tolerance, 10 ppm; fragment mass tolerance, 0.6 Da; minimum peptide length, 5; identification fidelity, <1% FDR for peptides and proteins. Without alkylation to peptides, carbamidomethylation as a static modification is excluded during database search (e.g., for single-cell analysis).

4.5.2. Quantify protein abundances via label-free⁴³ or label-based strategies^{44,45}.

4.5.3. OPTIONAL: Annotate proteins for gene ontology. PantherDB⁴⁶, Reactome⁴⁷, or Xenbase²³ can be used.

4.5.4. OPTIONAL: Quantify protein abundance and differences in protein abundances across cell/tissue types using software packages/webtools, such as the Trans-Proteomic Pipeline⁴⁸, Perseus⁴⁹, and Orange⁵⁰.

NOTE: Additional considerations on experimental design and software options were reviewed elsewhere^{41,51}.

4.5.5. OPTIONAL: Evaluate the results further using knowledge bases, such as STRING⁵² and BioPlex Display⁵³ for known protein-protein interactions and PhosphoSiteplus⁵⁴ for phosphorylations. For analyzing motifs and domains that are represented in the proteome, use webtools such as Simple Modular Architecture Research (SMART)⁵⁵.

REPRESENTATIVE RESULTS

This protocol enabled the study of proteins in single cells and their lineages as they establish tissues in *X. laevis* embryos. Figure 1 illustrates one such application of the approach to study proteins in neural-tissue-fated cells and the newly induced neural ectoderm in the embryo. As shown in Figure 1A, the bioanalytical workflow integrated traditional tools of cell and developmental biology to identify, inject/aspirate cells, and collect specimens. Figure 1B shows microprobe sampling of the left dorsal-animal (D₁₁) cell in the 16-cell embryo *in vivo* using a microinjector; after the experiment, embryos successfully developed to tadpoles with normal anatomy⁵⁶. Large embryonic cells (~100–250 μm in diameter) were conducive to manual microdissection as well. Dissection of a right dorsal-animal midline (D₁₁) cell is illustrated from the 16-cell embryo in Figure 1C. The setup also permitted tracing a clonal trajectory by injecting a fluorescent tracer into the identified precursor. As shown in Figure 1D, the approach allowed to isolate clones arising from the left and right D₁₁₁ cells via tissue dissection or by fluorescence-activated cell sorting (FACS). The sample collection strategies described here are sufficiently scalable in space and time to study embryonic development in new details.

The bioanalytical workflow integrated HRMS technologies to improve sensitivity and quantification (Figure 2). The collected proteins were measured via a bottom-up proteomic approach. Optional fractionation of samples based on orthogonal chemistry (e.g., high-pH then low-pH reversed-phase LC) aided detection sensitivity. To separate peptides, CE was selected for trace amounts of samples (<<~100 ng) and nanoLC for limited amounts of materials (<<150 ng). Peptides were sequenced using ESI-HRMS. The detected proteins were quantified using label-free and label-based strategies. Simplification of sample processing for single-cell analysis, such as elimination of the typical steps of reduction and alkylation followed by CE analysis, facilitated the identification of ~400–800 different proteins. Among the reported proteins were many with important functional roles, such as chaperonin containing TCP1 subunit 3 (Cct3), voltage-dependent ion channel (Vdac2), and creatine kinase-brain (Ckb). Multivariate and statistical data models helped us^{10,57}

and others^{9,58} find previously unknown differences in the proteomic composition of select cells and tissues using the approaches summarized in this protocol. Notably, these HRMS measurements required no functioning probes or knowledge about the composition of the specimens ahead of time, supporting discoveries.

In a series of studies, the proteomic state of identified cells in developing embryos of *X. laevis* (Fig. 3) was quantified²¹. Figure 3A shows the detection of gene translational differences between D₁₁ cells that were dissected from different embryos¹⁰. Microsampling CE-ESI-HRMS allowed us to identify and quantify up to ~700 proteins from single cells²¹. The representative primary HRMS-MS/MS data on identifying ~400 cumulative proteins from technical duplicate measurements on a D11 cell in the embryo was deposited to PRIDE. The approach was scalable to smaller cells and embryos from other model organisms, such as zebrafish²¹. Scalability to smaller cell sizes allowed us to explore the spatiotemporal reorganization of the D₁₁ progeny from a live embryo as it developed in time. Figure 3B presents the use of this protocol to perform subcellular quantitative proteomics of identified cells in the 16-, 32-, 64-, and 128-cell embryos. Proteins were separated into four groups that displayed distinct abundance profiles over clonal development²¹.

This protocol allowed us to conduct spatial and temporal proteomics in identified, developing cell clones (Figure 4). Figure 4A demonstrates the application of the approach for labeling and isolating cell clones constituting two tissues with important roles in neural tissue development and patterning of the embryo. The majority of the Spemann organizer (SO) was traced by labeling the left and right D₁₁₂ and D₂₁₂ cells via injection of fluorescent dextran. In parallel, the neighboring dorsal-animal (D₁₁₁) cells were labeled to mark the majority of the neural ectoderm (NE). The tissues were dissected, and their protein content was analyzed following this protocol. nanoLC-ESI-HRMS returned up to 2,000 different proteins from the tissues, including signaling, such as the Wnt, Fgf, and Tgf β pathways. The representative primary HRMS-MS/MS data on identifying ~1,800 cumulative proteins from technical duplicate measurements on a pool of dissected SO tissues was deposited to PRIDE. The Wnt pathway ligand Wnt10a and Wntless (Wls), a membrane protein dedicated to the secretion of Wnt ligands, were detected only in the NE proteome. The Wnt pathway was found suppressed in the SO and may explain a lack of Wnt-interacting proteins detected in the SO. These results showcase the applicability of this protocol for studying lineage-specific differences within the embryo.

The diverse proteomic data serve as valuable information for the assessment of function. The proteomic data can be evaluated using canonical knowledge bases. As shown in Figure 4B, pathway analysis of dysregulated proteins showed overrepresented translation and energy metabolism in both the SO and the NE datasets in our recent studies. The NE proteome was enriched in proteins associated with nuclear transport of protein cargo in the cell, likely indicating downstream events following signaling in the newly established NE (Figure 4C). The enrichment analysis in Figure 4D found upregulation in translation initiation, RNA-binding, binding in the proteasome complex, suggesting a role for dynamic protein turnover developing SO. Cell lineage-guided HRMS proteomics is scalable in space and

time and sufficiently sensitive to help better understand the molecular organization of cells during normal and impaired development.

DISCUSSION

This protocol enables the characterization of protein expression in identified cell lineages in embryos of the *Xenopus* species. Stemming from HRMS, the methodology combines exquisite specificity in molecular identification, capability for multi-protein detection without molecular probes (usually hundreds to thousands of different proteins), and a capability for quantification. Adaptability to classical tools and workflows in cell and developmental (neuro)biology expand HRMS proteomics to exciting applications, including holistic characterization of stem cell differentiation in the vertebrate *X. laevis* embryo.

The steps describe cell lineage-guided proteomics in the *X. laevis* embryo. As examples, we demonstrate the analysis of neural-fated single cells and their lineages and provide the corresponding CE- and nanoLC HRMS datasets through a public data repository (see PRIDE). This approach is readily adaptable to studies on the spatiotemporal regulation of proteins in multiple cell types (and lineages). Spatiotemporally guided proteomics in the developing embryo can also be extended to transcriptomic and metabolomic studies to promote the molecular systems biology understanding of cell differentiation and development of key organs, such as the nervous system.

This protocol adds new dimensions to bioanalysis. Cell cultures, such as the induced pluripotent stem cells (iPSCs)^{1,2}, facilitate the measurement of temporal proteome dynamics during cell differentiation. The approach detailed in this study peers into cell fate induction in the 3-dimensional live embryo, where complex morphogen gradients, parallel signaling pathways, and convergent extension processes collaborate to bring about tissue induction and morphogenesis. Studying proteome dynamics in the context of an embryo can provide information on parallel mechanisms that guide cell differentiation, an exciting direction to deepen understanding of differentiation and development.

The approach described here borrows the experimental benefits of the *Xenopus species* to this end, *X. laevis* in particular. Each cell of the early 16- and 32- cell *X. laevis* embryo is mapped to reproducible tissue fates in the adult organism, essentially a spatial projection of cells in the cleavage stage embryos. Reproducibility for cell-guided proteomics builds on accurate cell typing. We aid success by credentialing embryos for stereotypical pigmentation and cleavage before proceeding to experiments describing cell dissection and lineage tracing^{16,20}. It is important to note that cells of cleavage stage embryos often contribute to the formation of different tissue types to various degrees; the details of their level contribution to each tissue type is available on Xenbase²³. The embryonic stage and precursor cells to be lineage traced should therefore be chosen based on the biological question at hand. When culturing embryos over longer periods of time (e.g., >1 d), care ought to be taken to remove damaged/dead embryos, which may, in turn, diminish viability for the other embryos in the population.

For successful HRMS proteomics, careful attention should be paid to the analytical foundations of cell/tissue collection, protein extraction, and HRMS measurement. Because *Xenopus* embryos are cultured in media containing high concentrations of nonvolatile salts that are known to reduce HRMS sensitivity, it is recommended to reduce the aspirated media when collecting the cells and tissues for proteomic studies. It is a good practice to explore desalting to advance the identification and quantification of the proteins. Prior to HRMS measurement, the analytical performance of the CE- and LC-ESI-HRMS instruments should be evaluated, including separation, ionization, reproducibility, and linear dynamic range of quantification. With good analytical metrics, this protocol helps reduce animal usage in biological research, aids sensitivity for obtaining more powerful sets of biochemical data (Big Data), and enhances the power of statistical data analysis to interpret results. By default, we analyze each biological replicate in at least 3 technical replicates using CE or LC-HRMS, which are used to evaluate technical reproducibility and deepen the coverage of the detectable proteome. Power analysis helps the estimation of statistical power and design of the biological replicate size. The use of different sets of parent frogs is advised to account for naturally occurring biological variability among embryos.

ACKNOWLEDGMENTS

We thank Vi M. Quach and Camille Lombard-Banek for assistance with sample preparation and data collection in previous studies exemplifying the proteomic applications that are highlighted in this protocol. This work was partially supported by the National Science Foundation under award number IOS-1832968 CAREER (to P.N.), the National Institutes of Health under award number R35GM124755 (to P.N.), the University of Maryland–National Cancer Institute Partnership Program, and COSMOS Club Foundation research awards (to A.B.B. and L.R.P.).

REFERENCES

1. Shoemaker LD & Kornblum HI Neural Stem Cells (NSCs) and Proteomics. *Molecular & Cellular Proteomics*. 15 (2), 344–354, doi:10.1074/mcp.O115.052704, (2016). [PubMed: 26494823]
2. Cervenka J et al. Proteomic Characterization of Human Neural Stem Cells and Their Secretome During in vitro Differentiation. *Frontiers in Cellular Neuroscience*. 14 1–20, doi:10.3389/fncel.2020.612560, (2021).
3. Christian JL Morphogen Gradients in Development: From Form to Function. *Wiley Interdisciplinary Reviews–Developmental Biology*. 1 (1), 3–15, doi:10.1002/wdev.2, (2012). [PubMed: 23801664]
4. Gurdon JB, Elsdale TR & F. M Sexually mature individuals of *Xenopus laevis* from the transplantation of single somatic nuclei. *Nature*. 182, 64–65, doi:10.1038/182064a0, (1958). [PubMed: 13566187]
5. Harland RM & Grainger RM *Xenopus* research: metamorphosed by genetics and genomics. *Trends in Genetics*. 27 (12), 507–515, doi:10.1016/j.tig.2011.08.003, (2011). [PubMed: 21963197]
6. Moody SA Fates of the blastomeres of the 16-cell stage *Xenopus* embryo. *Developmental Biology*. 119 (2), 560–578, doi:10.1016/0012-1606(87)90059-5, (1987). [PubMed: 3803718]
7. Moody SA Fates of the blastomeres of the 32-cell stage *Xenopus* embryo. *Developmental Biology*. 122 (2), 300–319, doi:10.1016/0012-1606(87)90296-x, (1987). [PubMed: 3596014]
8. Dale L & Slack JMW Fate map for the 32-cell stage of *Xenopus laevis*. *Development*. 99 (4), 527–551 (1987). [PubMed: 3665770]
9. Sun LL et al. Single cell proteomics using frog (*Xenopus laevis*) blastomeres isolated from early stage embryos, which form a geometric progression in protein content. *Analytical Chemistry*. 88 (13), 6653–6657, doi:10.1021/acs.analchem.6b01921, (2016). [PubMed: 27314579]
10. Lombard-Banek C, Moody SA & Nemes P Single-cell mass spectrometry for discovery proteomics: quantifying translational cell heterogeneity in the 16-cell frog (*Xenopus*) embryo.

- Angewandte Chemie-International Edition. 55 (7), 2454–2458, doi:10.1002/anie.201510411, (2016). [PubMed: 26756663]
11. Zhang YY, Fonslow BR, Shan B, Baek MC & Yates JR Protein analysis by shotgun/bottom-up proteomics. *Chemical Reviews*. 113 (4), 2343–2394, doi:10.1021/cr3003533, (2013). [PubMed: 23438204]
 12. Sive HL, Grainger RM & Harland RM Early development of *Xenopus laevis*: a laboratory manual. Cold Spring Harbor Laboratory Press. (2000).
 13. Briggs JA et al. The dynamics of gene expression in vertebrate embryogenesis at single-cell resolution. *Science*. 360 (6392), 1–23, doi:10.1126/science.aar5780, (2018).
 14. Gupta M, Sonnett M, Ryazanova L, Presler M & Wuhr M in *Xenopus: Methods and Protocols* Vol. 1865 *Methods in Molecular Biology* (ed Vleminckx K) 175–194 (Humana Press Inc, 2018). [PubMed: 30151767]
 15. Baxi AB, Lombard-Banek C, Moody SA & Nemes P Proteomic characterization of the neural ectoderm fated cell clones in the *Xenopus laevis* embryo by high-resolution mass spectrometry. *ACS Chemical Neuroscience*. 2064–2073, doi:10.1021/acscemneuro.7b00525, (2018). [PubMed: 29578674]
 16. Moody SA Cell lineage analysis in *Xenopus* embryos. *Methods in Molecular Biology*. 135 331–347, doi:10.1385/1-59259-685-1:331, (2000). [PubMed: 10791329]
 17. Sater AK & Moody SA Using *Xenopus* to understand human diseases and developmental disorders. *Genesis*. 55 (1-2), 1–14, doi:10.1002/dvg.22997, (2017).
 18. Lombard-Banek C, Choi SB & Nemes P in *Enzyme Activity in Single Cells* Vol. 628 *Methods in Enzymology* eds Allbritton NL & Kovarik ML) 263–292 (2019). [PubMed: 31668233]
 19. Lombard-Banek C, Moody SA & Nemes P High-sensitivity mass spectrometry for probing gene translation in single embryonic cells in the early frog (*Xenopus*) embryo. *Frontiers in Cell and Developmental Biology*. 4 11, doi:10.3389/fcell.2016.00100, (2016). [PubMed: 26942179]
 20. Onjiko RM, Portero EP, Moody SA & Nemes P Microprobe capillary electrophoresis mass spectrometry for single-cell metabolomics in live frog (*Xenopus laevis*) embryos. *Jove-Journal of Visualized Experiments*. (130), 1–9, doi:10.3791/56956, (2017).
 21. Lombard-Banek C, Moody SA, Manzin MC & Nemes P Microsampling capillary electrophoresis mass spectrometry enables single-cell proteomics in complex tissues: developing cell clones in live *Xenopus laevis* and zebrafish embryos. *Analytical Chemistry*. 91 (7), 4797–4805, doi:10.1021/acs.analchem.9b00345, (2019). [PubMed: 30827088]
 22. Klein SL The first cleavage furrow demarcates the dorsal-ventral axis in *Xenopus* embryos. *Developmental Biology*. 120 (1), 299–304, doi:10.1016/0012-1606(87)90127-8, (1987). [PubMed: 3817297]
 23. Karimi K et al. Xenbase: a genomic, epigenomic and transcriptomic model organism database. *Nucleic Acids Research*. 46 (D1), D861–D868, doi:10.1093/nar/gkx936, (2018). [PubMed: 29059324]
 24. Kakebeen AD, Chitsazan AD & Wills AE Tissue disaggregation and isolation of specific cell types from transgenic *Xenopus* appendages for transcriptional analysis by FACS. *Developmental Dynamics*. 250 (9), 1381–1392, doi:10.1002/dvdy.268, (2021). [PubMed: 33137227]
 25. Garcia BA What does the future hold for top down mass spectrometry? *Journal of the American Society for Mass Spectrometry*. 21 (2), 193–202, doi:10.1016/j.jasms.2009.10.014, (2010). [PubMed: 19942451]
 26. Toby TK, Fornelli L & Kelleher NL in *Annual Review of Analytical Chemistry* Vol. 9 *Annual Review of Analytical Chemistry* eds Bohn PW & Pemberton JE 499–519 (2016).
 27. Zhang ZB, Dubiak KM, Huber PW & Dovichi NJ Miniaturized filter-aided sample preparation (MICRO-FASP) method for high throughput, ultrasensitive proteomics sample preparation reveals proteome asymmetry in *Xenopus laevis* Embryos. *Analytical Chemistry*. 92 (7), 5554–5560, doi:10.1021/acs.analchem.0c00470, (2020). [PubMed: 32125139]
 28. Wisniewski JR in *Microbial Proteomics: Methods and Protocols* Vol. 1841 *Methods in Molecular Biology* (ed Becher D) 3–10 (Humana Press Inc, 2018). [PubMed: 30259475]
 29. Hughes CS et al. Single-pot, solid-phase-enhanced sample preparation for proteomics experiments. *Nature Protocols*. 14 (1), 68–85, doi:10.1038/s41596-018-0082-x, (2019). [PubMed: 30464214]

30. Zhu Y et al. Nanodroplet processing platform for deep and quantitative proteome profiling of 10-100 mammalian cells. *Nature Communications*. 9 1–10, doi:10.1038/s41467-018-03367-w, (2018).
31. Wessel D & Flugge UI A method for the quantitative recovery of protein in dilute-solution in the presence of detergents and lipids. *Analytical Biochemistry*. 138 (1), 141–143, doi:10.1016/0003-2697(84)90782-6, (1984). [PubMed: 6731838]
32. Jiang L, He L & Fountoulakis M Comparison of protein precipitation methods for sample preparation prior to proteomic analysis. *Journal of Chromatography A*. 1023 (2), 317–320, doi:10.1016/j.chroma.2003.10.029, (2004). [PubMed: 14753699]
33. Hildonen S, Halvorsen TG & Reubsaet L Why less is more when generating tryptic peptides in bottom-up proteomics. *Proteomics*. 14 (17–18), 2031–2041, doi:10.1002/pmic.201300479, (2014). [PubMed: 25044798]
34. Budnik B, Levy E, Harmange G & Slavov N SCoPE-MS: mass spectrometry of single mammalian cells quantifies proteome heterogeneity during cell differentiation. *Genome Biology*. 19 1–12, doi:10.1186/s13059-018-1547-5, (2018). [PubMed: 29301551]
35. Drouin N et al. Capillary electrophoresis-mass spectrometry at trial by metabo-ring: effective electrophoretic mobility for reproducible and robust compound annotation. *Analytical Chemistry*. 92 (20), 14103–14112, doi:10.1021/acs.analchem.0c03129, (2020). [PubMed: 32961048]
36. Sun LL, Zhu GJ, Zhang ZB, Mou S & Dovichi NJ Third-generation electrokinetically pumped sheath-flow nanospray interface with improved stability and sensitivity for automated capillary zone electrophoresis-mass spectrometry analysis of complex proteome digests. *Journal of Proteome Research*. 14 (5), 2312–2321, doi:10.1021/acs.jproteome.5b00100, (2015). [PubMed: 25786131]
37. DeLaney K, Sauer CS, Vu NQ & Li LJ Recent advances and new perspectives in capillary electrophoresis-mass spectrometry for single cell "omics". *Molecules*. 24 (1), 21, doi:10.3390/molecules24010042, (2019).
38. Nemes P, Rubakhin SS, Aerts JT & Sweedler JV Qualitative and quantitative metabolomic investigation of single neurons by capillary electrophoresis electrospray ionization mass spectrometry. *Nature Protocols*. 8 (4), 783–799, doi:10.1038/nprot.2013.035, (2013). [PubMed: 23538882]
39. Choi SB, Zamarbide M, Manzini MC & Nemes P Tapered-tip capillary electrophoresis nano-electrospray ionization mass spectrometry for ultrasensitive proteomics: the mouse cortex. *Journal of the American Society for Mass Spectrometry*. 28 (4), 597–607, doi:10.1007/s13361-016-1532-8, (2017). [PubMed: 27853976]
40. Pino LK, Rose J, O'Broin A, Shah S & Schilling B Emerging mass spectrometry-based proteomics methodologies for novel biomedical applications. *Biochemical Society Transactions*. 48 (5), 1953–1966, doi:10.1042/bst20191091, (2020). [PubMed: 33079175]
41. Chen C, Hou J, Tanner JJ & Cheng JL Bioinformatics methods for mass spectrometry-based proteomics data analysis. *International Journal of Molecular Sciences*. 21 (8), 25, doi:10.3390/ijms21082873, (2020).
42. Peshkin L et al. On the relationship of protein and mRNA dynamics in vertebrate embryonic development. *Developmental Cell*. 35 (3), 383–394, doi:10.1016/j.devcel.2015.10.010, (2015). [PubMed: 26555057]
43. Cox J et al. Accurate proteome-wide label-free quantification by delayed normalization and maximal peptide ratio extraction, termed MaxLFQ. *Molecular & Cellular Proteomics*. 13 (9), 2513–2526, doi:10.1074/mcp.M113.031591, (2014). [PubMed: 24942700]
44. Gygi SP et al. Quantitative analysis of complex protein mixtures using isotope-coded affinity tags. *Nature Biotechnology*. 17 (10), 994–999, doi:10.1038/13690, (1999).
45. Thompson A et al. Tandem mass tags: A novel quantification strategy for comparative analysis of complex protein mixtures by MS/MS. *Analytical Chemistry*. 75 (8), 1895–1904, doi:10.1021/ac0262560, (2003). [PubMed: 12713048]
46. Mi HY et al. PANTHER version 16: a revised family classification, tree-based classification tool, enhancer regions and extensive api. *Nucleic Acids Research*. 49 (D1), D394–D403, doi:10.1093/nar/gkaa1106, (2021). [PubMed: 33290554]

47. Schmidt E et al. in On the Move Federated Workshops. 710–719 (Springer-Verlag Berlin, 2006).
48. Deutsch EW et al. Trans-Proteomic pipeline, a standardized data processing pipeline for large-scale reproducible proteomics informatics. *Proteomics Clinical Applications*. 9 (7-8), 745–754, doi:10.1002/prca.201400164, (2015). [PubMed: 25631240]
49. Tyanova S et al. The Perseus computational platform for comprehensive analysis of (prote)omics data. *Nature Methods*. 13 (9), 731–740, doi:10.1038/nmeth.3901, (2016). [PubMed: 27348712]
50. Demsar J et al. Orange: Data Mining Toolbox in Python. *Journal of Machine Learning Research*. 14 2349–2353 (2013).
51. Oberg AL & Vitek O Statistical Design of Quantitative Mass Spectrometry-Based Proteomic Experiments. *Journal of Proteome Research*. 8 (5), 2144–2156, doi:10.1021/pr8010099, (2009). [PubMed: 19222236]
52. Jensen LJ et al. STRING 8 — a global view on proteins and their functional interactions in 630 organisms. *Nucleic Acids Research*. 37 D412–D416, doi:10.1093/nar/gkn760, (2009). [PubMed: 18940858]
53. Schwappe DK, Huttlin EL, Harper JW & Gygi SP BioPlex Display: an interactive suite for large-scale AP-MS protein-protein interaction data. *Journal of Proteome Research*. 17 (1), 722–726, doi:10.1021/acs.jproteome.7b00572, (2018). [PubMed: 29054129]
54. Hornbeck PV et al. PhosphoSitePlus, 2014: mutations, PTMs and recalibrations. *Nucleic Acids Research*. 43 (D1), D512–D520, doi:10.1093/nar/gku1267, (2015). [PubMed: 25514926]
55. Letunic I, Khedkar S & Bork P SMART: recent updates, new developments and status in 2020. *Nucleic Acids Research*. 49 (D1), D458–D460, doi:10.1093/nar/gkaa937, (2021). [PubMed: 33104802]
56. Lombard-Banek C et al. In vivo subcellular mass spectrometry enables proteo-metabolomic single-cell systems biology in a chordate embryo developing to a normally behaving tadpole (*X. laevis*). *Angewandte Chemie-International Edition*. 60 (23), 12852–12858, doi:10.1002/anie.202100923, (2021). [PubMed: 33682213]
57. Lombard-Banek C, Reddy S, Moody SA & Nemes P Label-free quantification of proteins in single embryonic cells with neural fate in the cleavage-stage frog (*Xenopus laevis*) embryo using capillary electrophoresis electrospray ionization high-resolution mass spectrometry (CE-ESI-HRMS). *Molecular & Cellular Proteomics*. 15 (8), 2756–2768, doi:10.1074/mcp.M115.057760, (2016). [PubMed: 27317400]
58. Saha-Shah A et al. Single cell proteomics by data-independent acquisition to study embryonic asymmetry in *Xenopus laevis*. *Analytical Chemistry*. 91 (14), 8891–8899, doi:10.1021/acs.analchem.9b00327, (2019). [PubMed: 31194517]
59. Onjiko RM, Portero EP, Moody SA & Nemes P In situ microprobe single-cell capillary electrophoresis mass spectrometry: metabolic reorganization in single differentiating cells in the live vertebrate (*Xenopus laevis*) embryo. *Analytical Chemistry*. 89 (13), 7069–7076, doi:10.1021/acs.analchem.7b00880, (2017). [PubMed: 28434226]
60. Perez-Riverol Y et al. The PRIDE database and related tools and resources in 2019: improving support for quantification data. *Nucleic Acids Research*. 47 (D1), D442–D450, doi:10.1093/nar/gky1106, (2019). [PubMed: 30395289]

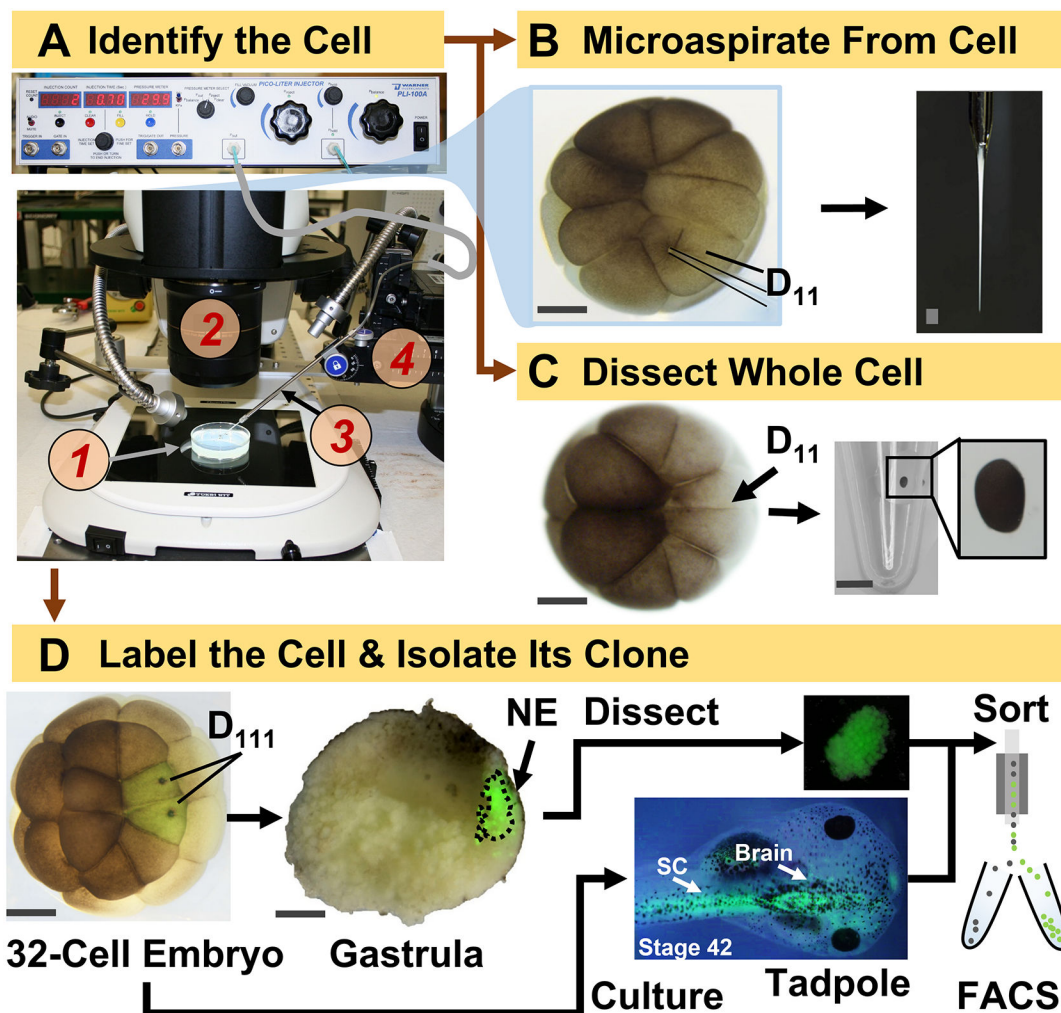


Figure 1: Spatiotemporally scalable proteomics enabling cell-lineage guided HRMS proteomics in the developing (frog) embryo.

(A) Visualization of the specimen (1) using a stereomicroscope (2) for injection of an identified cell (inset), using a micropipette (3) under control by a translation-stage (4). (B) Subcellular sampling of the identified left D₁₁ cell in a 16-cell embryo. (C) Dissection of a whole D₁₁ cell from a 16-cell embryo. (D) Fluorescent (green) tracing of the left and right D₁₁₁ progenies from a 32-cell embryo to guide dissection of the neural ectoderm (NE) in the gastrula (stage 10) and isolation of the descendent tissue from the tadpole using FACS. Scale bars: 200 μm for embryos, 1.25 mm for the vial. Figures were adapted with permission from references^{15,19,21,59}.

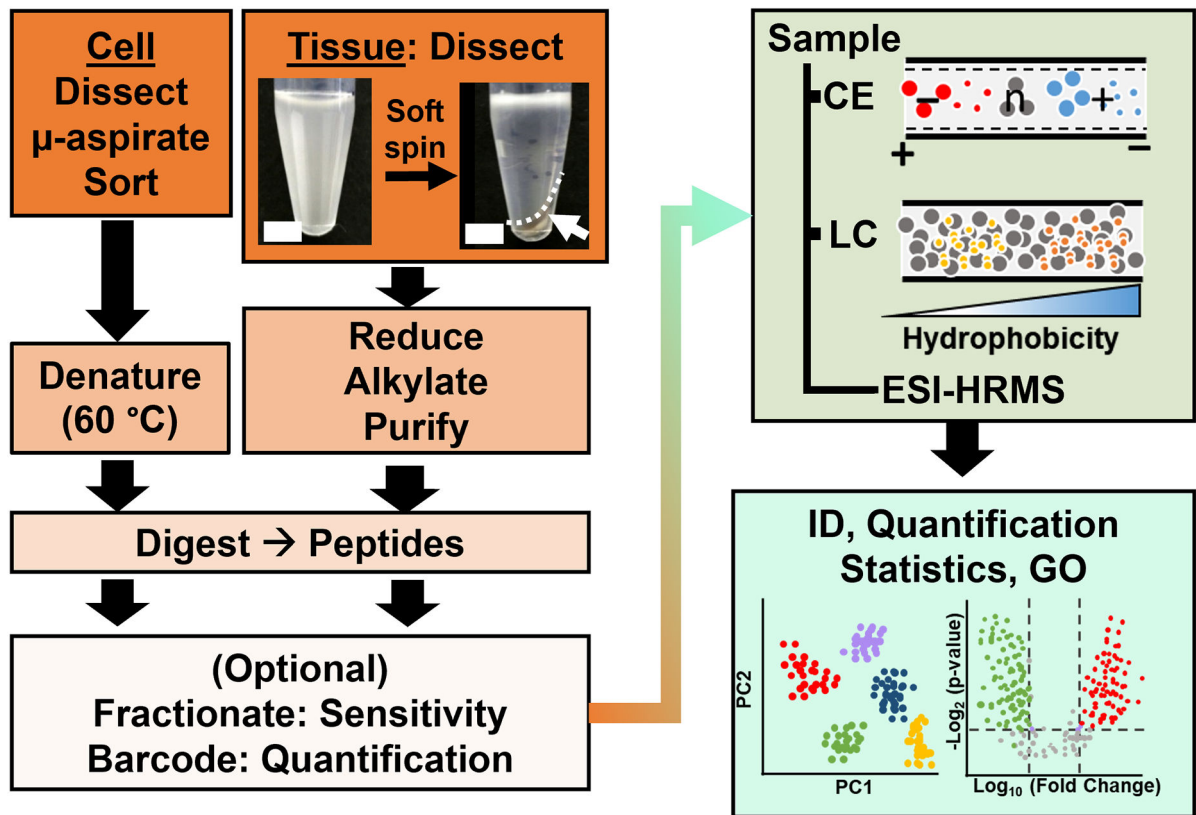


Figure 2: The bioanalytical workflow.

Micro-dissection and capillary aspiration, or FACS facilitated sampling of cellular and clonal protein content. Depletion of abundant yolk proteins and separation by capillary electrophoresis (CE) or nano-flow liquid chromatography (LC) enhanced detection sensitivity using electrospray ionization (ESI) high-resolution mass spectrometry (HRMS). Quantification revealed dysregulation, supplying new information for hypothesis-driven studies. Figures were adapted with permission from references¹⁵.

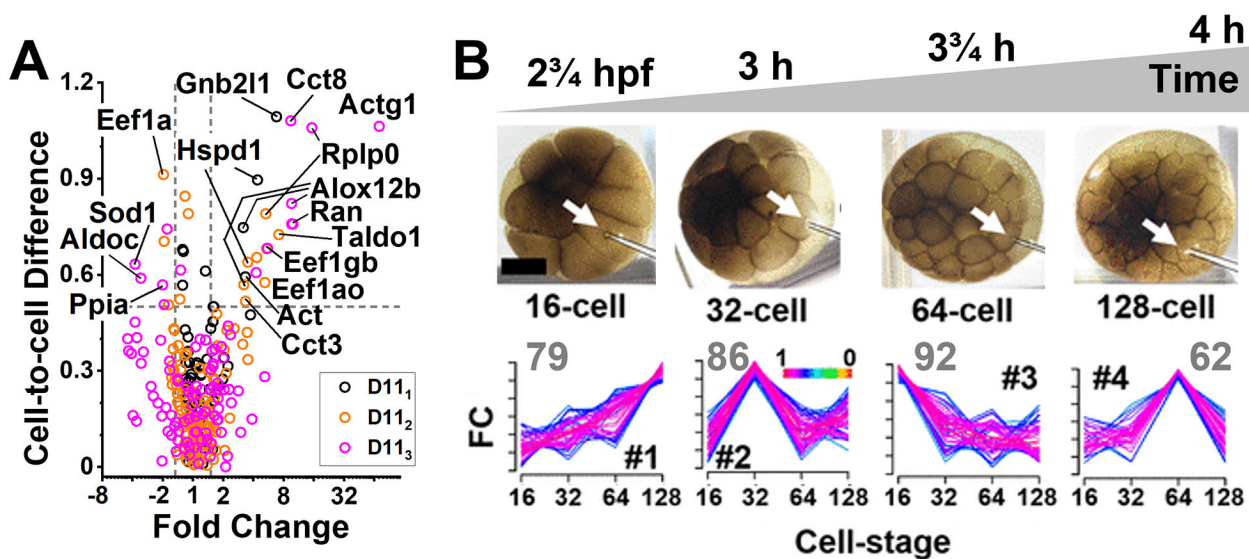


Figure 3: Protocol scalability from the subcellular space to clonal tissues in *X. laevis* embryo. (A) Measurement of proteomic differences between identified whole D₁₁ cells, revealing cell-cell heterogeneity. Gene names shown for select proteins. (B) Reorganization of the cellular proteome in the developing D₁₁ cell clone. Fuzzy C-means cluster analysis (GProx) of quantitative protein dynamics, grouping proteins based on similar expression patterns. Gray numbers show the number of different proteins that were quantified in each cluster. Figures were adapted with permission from references^{21,57}.

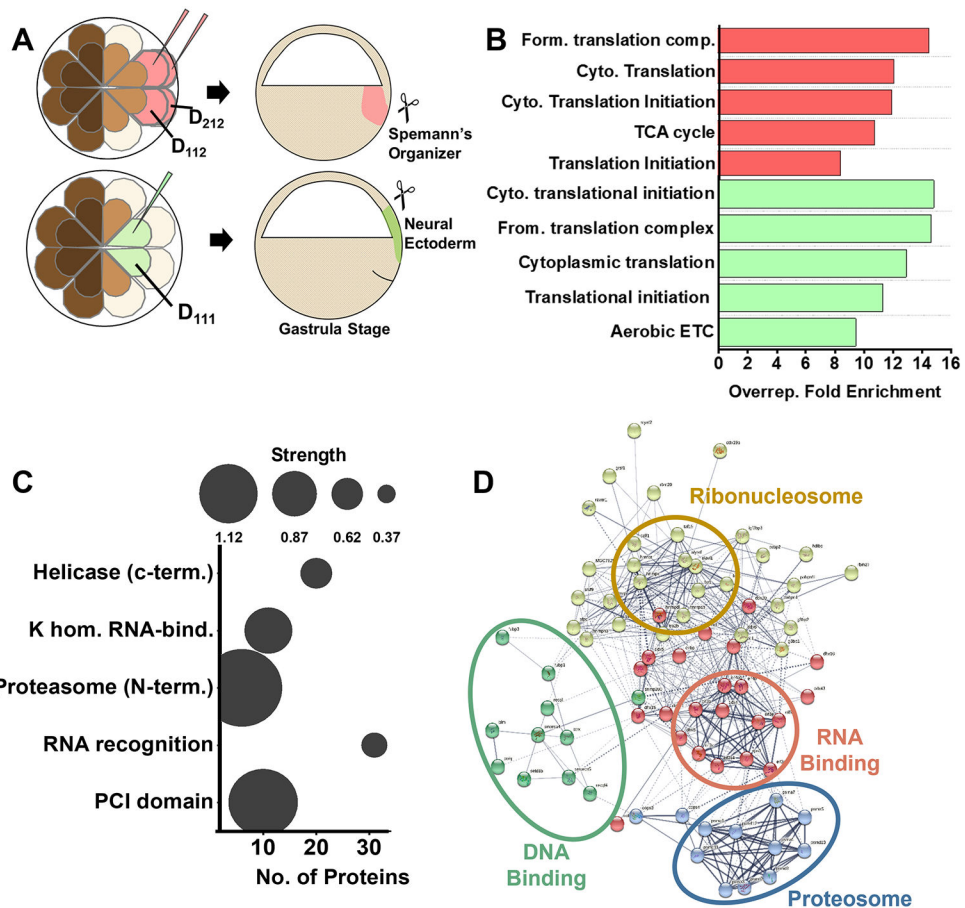


Figure 4: Example of data analysis from spatial tissue proteomics in the *X. laevis* embryos. (A) Differential labeling of the Spemann's Organizer (SO) and the neural ectoderm (NE) tissues by injection of fluorescent protein mRNA in the predecessor D₁₁₂ and D₂₁₂ in the 32-cell embryo, respectively. (B) Top 5 overrepresented biological processes in the SO (red) and NE (green) proteome showing detectable differences. Pathway overrepresentation analysis shows biological processes using Bonferroni correction. (C) Protein domain enrichment analysis (SMART), revealing enrichment of DNA and RNA binding motif-containing proteins in the SO. (D) STRING analysis predicting canonical protein-protein interactions based on the detected SO proteome.

Materials

Name	Company	Catalog Number	Comments
Acetonitrile (LC-MS-grade)	Fisher Scientific	A955	
Agarose	ThermoFisher Scientific	R0492	
Ammonium bicarbonate	Fisher Scientific	A643-500	
Analytical Column	Thermo Scientific	164941	
Analytical microbalance	Mettler-Toledo	XSE105DU	
Automatic peptide fractionation platform	Agilent	1260 Infinity II	
Borosilicate Capillaries	Sutter Instruments Co.	B100-50-10	
Borosilicate Capillaries (for making Emitters)	Sutter Instruments	B100-75-10	
C18 spin columns (for desalting)	ThermoFisher Scientific	89870	
Camera to monitor electrospray	Edmund Optics Inc.	EO-2018C	
Combretastatin A4	Millipore Sigma	C7744	
Commercial CESI system	AB SCIEX	CESI	
(Cyclohexylamino)-1-propanesulfonic acid (CAPS)	VWR	97061-492	
Cytochalasin D	Millipore Sigma	C8273	
Dextran, Alexa Fluor 488; 10,000 MW, Anionic, Fixable	ThermoFisher Scientific	D22910	
Diothiothreitol	Fisher Scientific	FERR0861	
Dumont #5 Forceps	Fine Science Tools	11252-30	
EDTA	Fisher Scientific	AAJ62786AP	
Epifluorescence light source	Lumencore	AURA III	
Eppendorf LoBing microcentrifuge tubes: protein	Fisher Scientific	13-698-793	
Formic acid (LC-MS-grade)	Fisher Scientific	A117-50	
Freezer (-20 °C)	Fisher Scientific	97-926-1	
Freezer (-80 °C)	Thermo Scientific	TSX40086A	
Fused silica capillary	Molex	1088150596	
Heat Block	Benchmark	BSH300	
High pressure liquid Chromatography System	ThermoFisher Scientific	Dionex Ultimate 3000 RSLC nanosystem	
High voltage power supply	Spellman	CZE1000R	
High-resolution Mass Spectrometer	ThermoFisher Scientific	Orbitrap Fusion Lumos Tribrid Mass Spectrometer	
HPLC caps	Thermo Scientific	C4013-40A	
HPLC Vials	Thermo Scientific	C4013-11	
Illuminator e.g. Goosenecks	Nikon	C-FLED2	
Ingenuity Pathway Analysis	Qiagen		
Iodoacetamide	Fisher Scientific	AC122275000	
Methanol (LC-MS-grade)	Fisher Scientific	A456	
Methanol (LC-MS-grade)	Fisher Scientific	A456-4	
Microcapillary puller	Sutter Instruments	P-2000	

Name	Company	Catalog Number	Comments
Microinjector	Warner Instrument, Hamden, CT	PLI-100A	
Micropipette puller	Sutter Instruments Co.	P-1000	
MS data analysis software, commercial	ProteomeDiscoverer		
MS data analysis software, opensource	MaxQuant		
non-idet 40 substitute	Millipore Sigma	11754599001	
Petri dish 60 mm and 80 mm	Fisher Scientific	S08184	
Pierce 10 μ L bed Zip-tips (for desalting)	ThermoFisher Scientific	87782	
Pierce bicinchoninic acid protein assay kit	ThermoFisher Scientific	23225	
Pierce quantitative colorimetric peptide assay	ThermoFisher Scientific	23275	
Pierce Trypsin Protease (MS Grade)	Fisher Scientific	PI90058	
Protein LoBind vials	Eppendorf	0030108434 , 0030108442	
Refrigerated Centrifuge	Eppendorf	5430R	
Refrigerated Incubator	Thermo Scientific	PR505755R/3721	
sodium isethionate	Millipore Sigma	220078	
sodium pyrophosphate	Sigma Aldrich	221368-100G	
Stainless steel BGE vial	Custom-Built		
Stainless steel sample vials	Custom-Built		
Stereomicroscope (objective 10x)	Nikon	SMZ 1270, SZX18	
Sucrose	VWR	97063-790	
Syringe pumps (2)	Harvard Apparatus	704506	
Syringes (gas-tight): 500–1000 μ L	Hamilton	1750TTL	
Transfer pipettes (Plastic, disposable)	Fisher Scientific	13-711-7M	
Trap Column	Thermo Scientific	164750	
Tris-HCl (1 M solution)	Fisher Scientific	AAJ22638AP	
Vacuum concentrator capable of operation at 4–10 $^{\circ}$ C	Labconco	7310022	
Vortex-mixer	Benchmark	BS-VM-1000	
Water (LC-MS-grade)	Fisher Scientific	W6	
Water (LC-MS-grade)	Fisher Scientific	W6	
XYZ translation stage	Thorlabs	PT3	
XYZ translation stage	Custom-Built		